

**Polytechnic
Institute
of New York**
MICROWAVE RESEARCH INSTITUTE
AFOSR-TR. 81-0567

(12)

REV. 1P

POLY-MRI-1412-80

October 1980

REVISED · May 1981

ADA102005

**CHANGE IN REFLECTIVITY OF METALS
UNDER INTENSE LASER RADIATION**

by

William T. Walter

Final Technical Report

DTIC
SELECTED
S JUL 24 1981
D
A

Prepared for

AIR FORCE OFFICE OF SCIENTIFIC RESEARCH

Grant No. AFOSR-78-3557

817 24 008

Approved for public release;
distribution unlimited.

Unclassified

SECURITY CLASSIFICATION OF THIS PAGE (When Data Entered)

REPORT DOCUMENTATION PAGE

READ INSTRUCTIONS
BEFORE COMPLETING FORM

1 AFOSR-TR- 81 - 0567

2. GOVT ACCESSION NO.

3. RECIPIENT CATALOG NUMBER

AD-A102005

9

4. TITLE (and Subtitle)

Change in Reflectivity of Metals Under
Intense Laser Radiation.

5. TYPE OF REPORT & PERIOD COVERED
FINAL, technical rept
1 April 78 - 30 September 80

6. AUTHOR(s)

William T. Walter

7. CONTRACT OR GRANT NUMBER(s)

14 AFOSR-78-3557

15 10 AFOSR-78-3557

9. PERFORMING ORGANIZATION NAME AND ADDRESS

Polytechnic Institute of New York
Microwave Research Institute
Route 110, Farmingdale, New York 11735

10. PROGRAM ELEMENT, PROJECT, TASK
AREA & WORK UNIT NUMBERS

61102F 2306/A2

11. CONTROLLING OFFICE NAME AND ADDRESS

Air Force Office of Scientific Research
Bolling Air Force Base, Bldg. 410
Washington, D. C. 20332

12. REPORT DATE 31 October 1980

13. NUMBER OF PAGES

38

14. MONITORING AGENCY NAME & ADDRESS (if different from Controlling Office)

15. SECURITY CLASS. (of this report)

Unclassified

16. DISTRIBUTION STATEMENT (of this Report)

15a. DECLASSIFICATION/DOWNGRADING
SCHEDULE

Approved for public release; distribution unlimited.

17. DISTRIBUTION STATEMENT (of the abstract entered in Block 20, if different from Report)

18. SUPPLEMENTARY NOTES

19. KEY WORDS (Continue on reverse side if necessary and identify by block number)

Reflectivity, reflectance, laser-material interaction, metals, copper,
lasers, Q-switched ruby laser, surface temperature.

20. ABSTRACT (Continue on reverse side if necessary and identify by block number)

The reflectance behavior of a target surface during laser irradiation determines the laser energy which is directly absorbed. Experimentally, the reflectance of a metal surface has been reported to undergo a sharp and substantial decrease during an intense laser pulse. Explanations have been offered based on an increase in electron-phonon collision frequency as the temperature of the metal surface rises to the melting point of the metal. For high conductivity metals such as copper, we have shown that the temperature dependence of a Drude-type free-electron model can not explain the substantial reflectance

Unclassified

SECURITY CLASSIFICATION OF THIS PAGE(When Data Entered)

changes reported. Three other classes of explanations have been proposed: 1) deformation of the metal surface, 2) plasma formation in the front of the target, or 3) a nonlinear process causing enhanced absorption within the metal. Specular and total reflectances of metal surfaces during ruby laser irradiation have been measured at the Polytechnic. The laser energy absorbed has been calculated and the temperature history of the metal surface determined using a one-dimensional heat-conduction approach. Reflectance and temperature histories have been related to permanent changes observed in the metal target surface. Only at temperatures significantly above the melting point of the metal does a substantial decrease in the total reflectance occur.

Unclassified

SECURITY CLASSIFICATION OF THIS PAGE(When Data Entered)

TABLE OF CONTENTS

	<u>Page</u>
I. INTRODUCTION	1
II. TARGET REFLECTANCE BEHAVIOR	3
III. FREE ELECTRON MODEL	6
IV. REFLECTANCE MEASUREMENTS	13
V. TEMPERATURE OF THE METAL SURFACE	19
VI. DISCUSSION	24
VII. PROBE LASER REFLECTANCE MEASUREMENTS	25
VIII. CONCLUSIONS	27
IX. REFERENCES	28
X. LIST OF PUBLICATIONS AND DISSERTATIONS	31
XI. LIST OF PERSONNEL INVOLVED IN RESEARCH	32
XII. LIST OF COUPLING ACTIVITIES	33

AIR FORCE OFFICE OF SCIENTIFIC RESEARCH (AFSC)
NOTICE OF TRANSMITTAL TO DDC

This technical report has been reviewed and is
approved for public release IAW AFR 190-12 (7b).
Distribution is unlimited.

A. D. BLOSE
Technical Information Officer

Approved for	<input type="checkbox"/>
DDA&I	<input type="checkbox"/>
TAB	<input type="checkbox"/>
Announced	<input type="checkbox"/>
Classification	<input type="checkbox"/>
Distribution	
Availability Codes	
Avail and/or	<input type="checkbox"/>
Special	<input type="checkbox"/>

A

I. INTRODUCTION

The development of a better understanding of the transfer of energy from an incoming laser beam to the target material it strikes is a research goal of the Wave-Matter Interaction Group at the Polytechnic. To accompany our ongoing theoretical research program we have begun an experimental program to measure parameters which monitor the state of the target material in real time on a nanosecond or faster time scale. Although we would like to be able to measure directly parameters such as the target surface temperature, for example, on such a time scale, it is extremely difficult to measure temperature directly even on a microsecond time scale. However, since the reflectance of the target can be measured in real time with subnanosecond resolution, it may be a crucial and process revealing parameter in following the transfer of energy from an intense laser beam to a metal target surface. For opaque targets such as metals, the absorbence is one minus the reflectance. Thus, the temporal behavior of their surface temperatures, which cannot be directly measured on such a fast time scale, can then be calculated from the measured reflectance.

At present, materials processing applications are usually carried out at incident laser power densities $< 10^7 \text{ W/cm}^2$ to avoid plasma formation at the target surface. The effect of a plasma has been unpredictable and difficult to control. When located close to the target, the plasma can enhance the coupling, and when further removed, it can completely shield the target from the laser. With a better understanding of the initiation and energy transfer processes during plasma formation, we may expect that materials processing applications could utilize the considerably higher power densities, as high as 10^{15} W/cm^2 , which are now available from lasers. Not only could applications of increasing scale be considered, but fluid dynamic effects could be utilized to make these processes more efficient.

Our aim then is to relate changes in the target's reflectance to physical changes taking place at the metal surface, such as surface deformation, slip, melting, plasma formation, ejection of liquid metal, etc. The reflectance behavior of a metal surface irradiated by an intense laser pulse must be consistent with the laser energy absorbed, the metal surface temperature attained, and the surface damage produced.

During this AFOSR program, we have measured both the specular and total reflectances of vapor-deposited copper surfaces during irradiation by a Q-switched ruby laser. We have calculated the laser energy absorbed and determined the temperature of the copper target surface using a one-dimensional heat conduction approach. Finally, we have related the reflectance and temperature histories to any permanent change or damage observed in the copper target material.

II. TARGET REFLECTANCE BEHAVIOR

Experimentally, the reflectance of a metal surface has been reported to undergo a sharp and substantial decrease during an intense laser pulse.¹⁻¹¹ For incident laser power densities above threshold values which lie between 10^7 and 10^9 W/cm^2 , the measured reflectance of a metal surface drops significantly before partially or totally recovering as indicated by the curves in Figure 1a. This type of reflectance change was first reported by Bonch-Bruevich et al.¹ during individual spikes $\sim 400\text{-ns FWHM}$ (Full Width at Half-Maximum intensity) within a millisecond $1.06\text{-}\mu\text{m Nd}$ glass laser pulse on targets of silver, copper, aluminum, dural and steel as indicated.

There are three distinct regions within a generalized reflectance curve as illustrated in Figure 1b: first, AB - an initial steep decrease to \sim one-half of the initial reflectance; second, BC or BC' - a plateau region during which the reflectance remains approximately constant; and third, C'D' - a complete reflectance recovery, or for higher intensity laser pulses CD, a further decrease to \sim one-tenth of the initial reflectance followed by a partial recovery.

Zavecz, Saifi and Notis⁴ reported similar reflectance curves during Q-switched $1.06\text{-}\mu\text{m Nd:YAG}$ laser pulses $\sim 60\text{-ns FWHM}$ on single crystal copper and tantalum targets as shown in Figure 1c. The remarkably close agreement between Zavecz's 0.64 plateau reflectance value and the 0.66

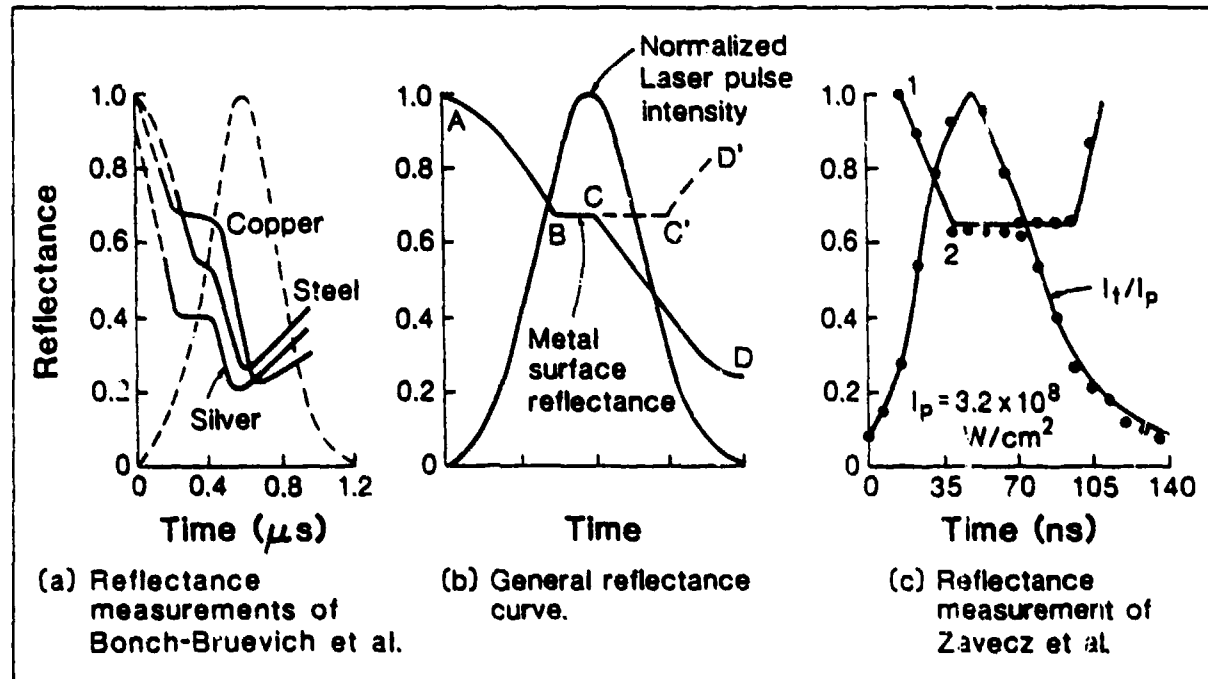


Fig. 1. Metal reflectance behavior during an intense laser pulse.

value of Bonch-Bruevich for copper, the only metal common to both investigations, is evident in Figure 1. Plateau features have also been reported by Dymshits,⁸ using a 30-ns FWHM 1.06- μ Nd glass single laser pulse on thin aluminum films, and Walters and Clauer,¹⁰ using gain-switched 50 to 70-ns 10.6- μ TEA CO₂ laser pulses on polished polycrystalline aluminum rods.

Bonch-Bruevich et al.¹ associated the initial steep decrease in the reflectance curve, AB, with the heating of the metal surface to melting and with the drop in electrical conductivity which accompanies melting. The plateau BC or BC', they suggested, indicated that the temperature of the molten layer remained constant while the absorbed radiant energy propagated a melting wave into the solid. The further reflectance drop during region CD was attributed to a decrease in the amount of energy conducted to the liquefaction wavefront and, therefore, indicated a second region of increasing surface temperature.

Zavecz et al.⁴ tested Bonch-Bruevich's conjecture that the metal was melting during region BC. A single-crystal copper target was irradiated with a laser intensity (3.2×10^8 W/cm²) which was sufficient to attain the plateau reflectance BC, as shown in Figure 1c, but not high enough to cause the second reflectance decrease. Examination of the target by scanning electron beam microscopy revealed no evidence of melting. Melting occurred during the second decrease in reflectance, CI of Figure 1b. A major difference between the two experiments was the use of an integrating sphere by Bonch-Bruevich and, therefore, a total reflectance measurement while Zavecz et al. measured only the specular reflectance. In ensuing experiments to Zavecz's, Koo and Slusher⁵ proposed that the reflected beam could have been deflected into a wide cone of angles by a transient grating structure produced on the metal target surface. Ready,⁶ using a 10.6- μ CO₂ laser, and von Allmen⁹ using a 1.06- μ Nd laser on metal targets, found substantial and permanent changes from specular to diffuse reflectance during the laser pulse. Ready used a probe laser to subtract plasma absorption and concluded that no recovery of reflectance occurred during or after the pulse. An ellipsoidal light collector was employed by von Allmen in front of a copper target in air. He found no significant change in the total reflectance until the metal surface exceeded the boiling point. Prokhorov et al.³ suggested the formation of a liquid dielectric layer causing an enhanced absorption. More recently,

Dymshits⁸ observed Figure 1-type reflectance changes during a specular reflectance measurement with the metal target film in vacuum. He suggested that the reflection takes place from a plasma formation in front of the metal surface. Walters and Clauer¹⁰ report a sharp decrease to ~ 0.35 in specular reflectance at the melting point of Al followed by nearly complete recovery. No luminosity was observed and no significant permanent loss of the high specular reflectivity was detected.

An understanding of the metal surface reflectance behavior during an intense laser pulse is lacking at present. In addition to Bonch-Bruevich's suggestion that the initial steep decrease in reflectance is associated with the heating of the metal surface to melting, three classes of alternate explanations have been offered for the steep decrease in metal target reflectance during an intense laser pulse: 1) surface deformation, 2) plasma formation, or 3) nonlinear process. Before discussing these, we shall first examine the change in reflectance expected when a metal is heated to its melting point.

III. FREE ELECTRON MODEL

The Fresnel expression for the reflectivity, R , of radiant intensity at normal incidence on the surface of a homogeneous substance is^{12, 13}

$$R = \frac{|\tilde{n} - 1|^2}{|\tilde{n} + 1|^2}$$

where \tilde{n} is the complex refractive index. From the viewpoint of optics, the complex index of refraction may be expressed in terms of the optical constants n and k of the material

$$\tilde{n} = n - ik$$

where n is the index of refraction and k is the extinction coefficient.

In the Drude or free electron model, a metal is viewed as a gas of free electrons which interacts with a background positive-ion lattice represented by phonons. The complex index of refraction then may be expressed in terms of the plasma frequency

$$\omega_p = \sqrt{4\pi Ne^2/m^*} ,$$

the average electron-phonon collision frequency $\equiv \nu_c$ and the frequency of the incident light $\omega_{\text{light}} \equiv 2\pi c/\lambda$,

$$\tilde{n} - 1 - \frac{\omega_p^2}{\omega_{\text{light}}^2 + \nu_c^2} \left(1 + i \frac{\nu_c}{\omega_{\text{light}}} \right) = 1 - \frac{1}{\omega^2 + \nu^2} \left(1 + i \frac{\nu}{\omega} \right)$$

where $\omega \equiv \omega_{\text{light}}/\omega_p$, and $\nu \equiv \nu_c/\omega_p$. Here N is the free electron density, e is the electronic charge, m^* is the effective mass of the free electron in the metallic lattice and $i \equiv \sqrt{-1}$. For visible light incident on a good conductor

$$\omega_p \approx 10^{16} \text{ sec}^{-1} > \omega_{\text{laser}} \approx 10^{15} \text{ sec}^{-1} > \nu_c \approx 10^{14} \text{ sec}^{-1} .$$

Therefore, $\omega \sim 10^{-1}$ and $\nu \sim 10^{-2}$.

When the temperature is raised to the melting point, no significant change in the free electron density is expected for a metal whose bandgap is much greater than the thermal energy change. Therefore, no appreciable

change is expected in the plasma frequency ω_p . The phonon density, however, may increase significantly and hence also may the electron-phonon collision frequency and ν . Figure 2 shows the dependence of the Fresnel reflectivity on the collision frequency for neodymium and ruby laser frequencies normally incident on a copper surface.

There has been considerable variation in the room-temperature reflectance measurements of many metals. Since the absorption depth, $\lambda/2\pi k$, is only a few hundred angstroms at most for metals in the visible-near infrared spectral region, the measured reflectances of metals are very sensitive to the method of preparation of the surface as well as to the history of the surface from preparation to measurement. When the metallic surface is produced by polishing, mechanical stress can deform the surface by producing an amorphous layer which may be several hundred angstroms thick.¹⁴ Even more detrimental is the embedding of polishing-compound particles which is more likely to take place in soft metals: copper, aluminum, etc. If an oxide layer is allowed to form, the reflectance measured will not be that of the pure metal. For metals which are good conductors and therefore also possess high reflectivities, processes which modify the metal-air or metal-vacuum interface generally reduce the reflectance. The highest reflectances of metals have been measured for evaporated coatings prepared in a high vacuum at a high rate of deposition of the metal and measured immediately after preparation while still in a high vacuum.¹⁵ Reflectances of Ag, Cu and Al measured under these conditions at 1.06μ are .994, .985, and .944, respectively.

Figure 2 indicates that for a room-temperature copper reflectivity of 0.985 at 1.06μ , the ratio of the electron-phonon collision frequency to the plasma frequency $\nu = 0.00749$. According to the free electron model then, for the reflectivity of copper to decrease to 75%, for example, ν must increase so that $\nu > 0.15$. This means an increase of more than 20 times in the electron-phonon collision frequency.

Ujihara¹³ has examined the temperature dependence of a Drude-type free-electron model for high conductivity metals. He asked whether the increase with temperature of the electron-phonon collision frequency can account for a reflectance decrease to the plateau value by the time that the metal reaches its melting point. Ujihara assumed a Debye model for the

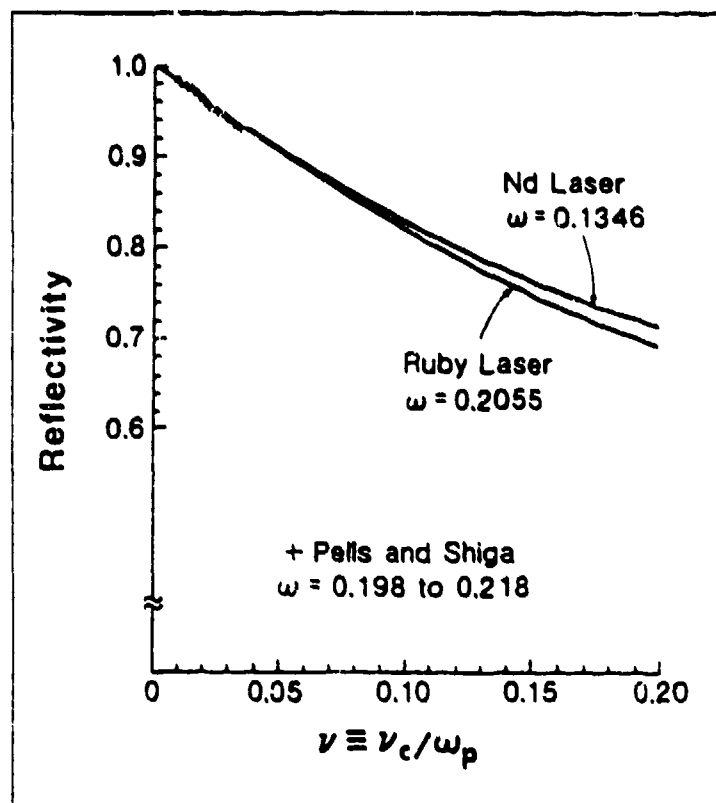


Fig. 2. Reflectivity of copper as a function of the electron-phonon collision frequency ν_c for two incident laser frequencies ω .

phonon spectrum and N-scattering processes on a spherical Fermi surface. Both the Debye temperature and the electron distribution were considered to be independent of temperature in the 300°K to melting point region. Ujihara's results for several metals at ruby and Nd wavelengths are shown in Figure 3. The reflectance of solid copper at 1.06μ decreases from 0.95 at room temperature to 0.73 at the melting point, 1356°K . Since the conductivity of copper, like many other metals, decreases by a factor of 2 upon melting,¹⁶ a reflectance of 0.58 would be expected for liquid copper at 1.06μ at the melting point. These reflectance values bracket the plateau reflectances of 0.66 and 0.64 observed by Bonch-Bruevich and Zavecz, and suggest that the Drude-type free-electron model may be able to explain the reflectance behavior observed. Indeed, as shown in Figure 4, Chan et al.⁷ claim to have confirmed Ujihara's theoretical reflectivity curves using a ruby laser on copper and aluminum targets and calculating the surface temperature on the basis of a one-dimensional heat flow model.

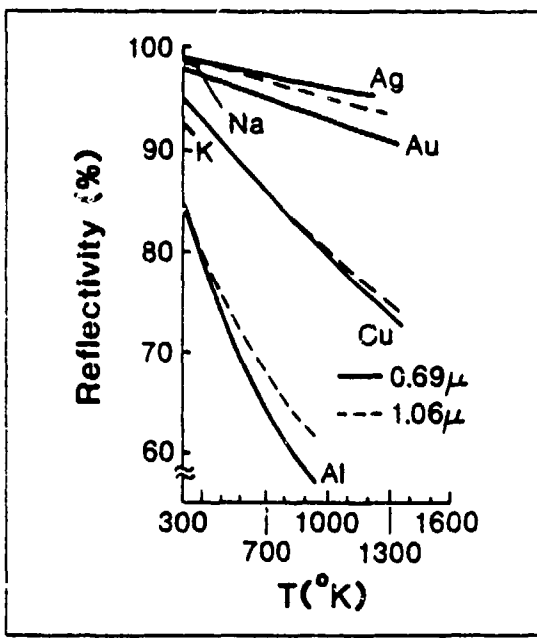


Fig. 3. Ujihara's calculated reflectivities (13) for several metals at two laser frequencies.

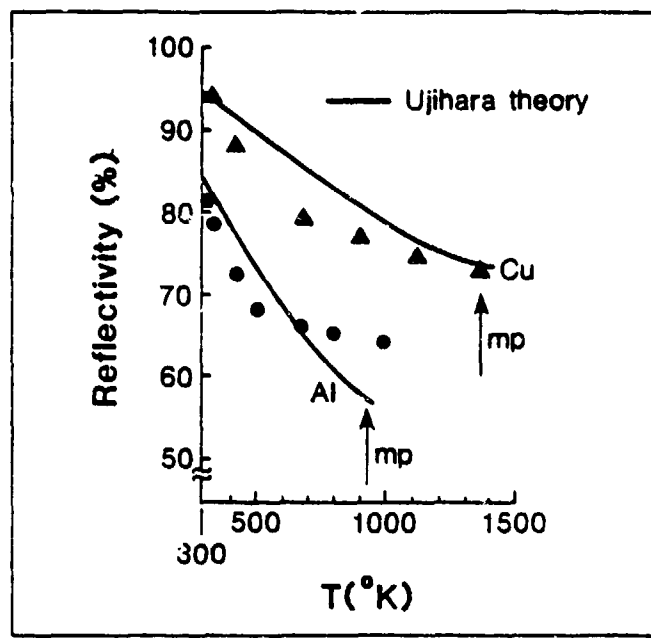


Fig. 4. Chan's measured reflectances (7) of copper (triangles) and aluminum (dots) at 0.69μ .

Ujihara's analysis has been examined by Walter,¹⁷ who pointed out that Ujihara, in his determination of the plasma frequency ω_p , used the 1913 effective-mass measurements.¹⁸ For copper, the old value is almost two times the more recent measurements. When the resulting low value for the plasma frequency was used with values of the optical constants, n and k , the room-temperature value Ujihara calculated for the electron-phonon collision frequency was 2.5 times too high and the room temperature reflectivity at 1.06μ was 95.2% instead of 98.5%. With these incorrect initial values, his analysis then predicted substantial changes in the collision frequency and in the reflectivity which are not confirmed by experiment, as indicated in Figure 5.

The solid curve in Figure 5 shows the temperature dependence of the reflectivity of copper calculated by Ujihara. The dotted curve extends Ujihara's analysis down to 77°K . The optical properties of copper have been measured polarimetrically in ultra-high vacuum ($\sim 10^{-9}$ Torr) by Pells and Shiga¹⁹ over the temperature range 77 to 920°K . Reflectances computed from Pells and Shiga's experimental values of n and k are also indicated in Figure 5. The discrepancy between theory and experiment is substantial.

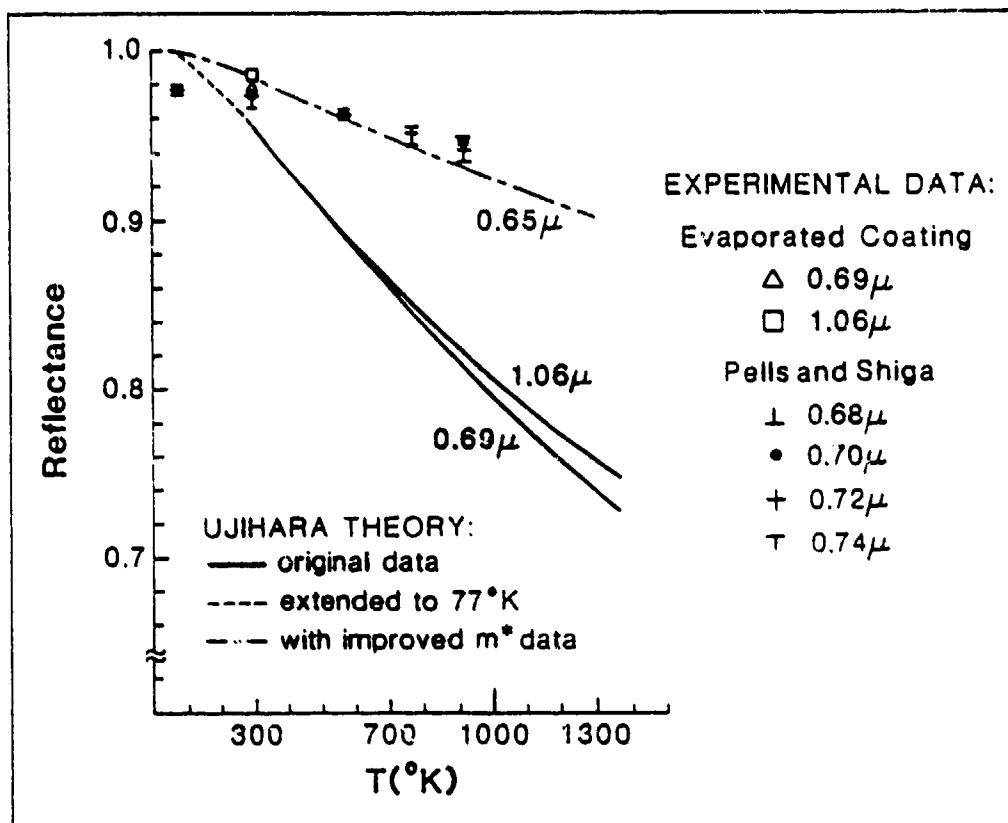


Fig. 5. Temperature dependence of the reflectance of copper.

However, when the improved data listed in Table 1 is used, then the theory of Ujihara is in much better agreement with Pells and Shiga's experimental results. The dominant change responsible for most of the improvement is Schulz's careful determination²⁰ of the effective electron mass in copper

Table 1. Input Data for Ujihara's Theory

Parameter		Original Ujihara Analysis	Improved Data of Reference 17
Index of refraction	n	0.150 ^a	0.1074 ^b
Extinction coefficient	k	4.049 ^a	3.9104 ^b
Wavelength	λ	0.70 μ ^a	0.65 μ ^b
Effective mass	m^*/m	2.56 ^c	1.45 ^d

^aReference 21.

^bReference 22.

^cReference 18.

^dReference 20.

including a correction for the anomalous skin effect. With these improvements in the input data used in the Ujihara theory, we may conclude:

- (1) the reflectance of liquid copper²³ is ~ 85%, not ~ 65%, and
- (2) it is unlikely that the temperature dependence of a Drude-type free-electron model can explain the substantial reflectance changes reported for high-conductivity metals such as copper¹⁷

In Figures 6a and 6b, the temperature dependence of the optical constants n and k , and the free-electron model constants ω_p and v_c , are displayed and compared with the polarimetric measurements of Peils and Shiga.¹⁹ As expected, it is evident that the plasma frequency does not change significantly with temperature. The plasma frequency can be determined from the optical constants n and k or from the free electron density and effective mass N and m^* . When the most precise n and k values²² are used to determine ω_p for Ag, Cu and Au, good agreement is obtained with ω_p values determined from N and m^* , using the effective mass values of Schulz. Also, the effective mass for electrons in Cu determined by Schulz from optical properties at 2μ is nearly identical to the value from electronic specific heat determinations.²⁰ It is also evident in Figure 6b that the electron-phonon collision frequency undergoes a much smaller increase (~4) when copper is heated from room temperature to its 1356°K melting point than that required (> 20) to produce the substantial reflectance drop to Figure 1-type plateau values.

Finally, it is clear from the plots of n and v_c in Figure 6 that even with the improved input data listed in Table 1, the theory of Ujihara does not have the correct functional dependence with temperature for either the index of refraction or the electron-phonon collision frequency for $T < 500^{\circ}\text{K}$. Refinements such as a departure from sphericity of the Fermi surface and more than one electron-phonon collision frequency could be considered to improve the Ujihara treatment.

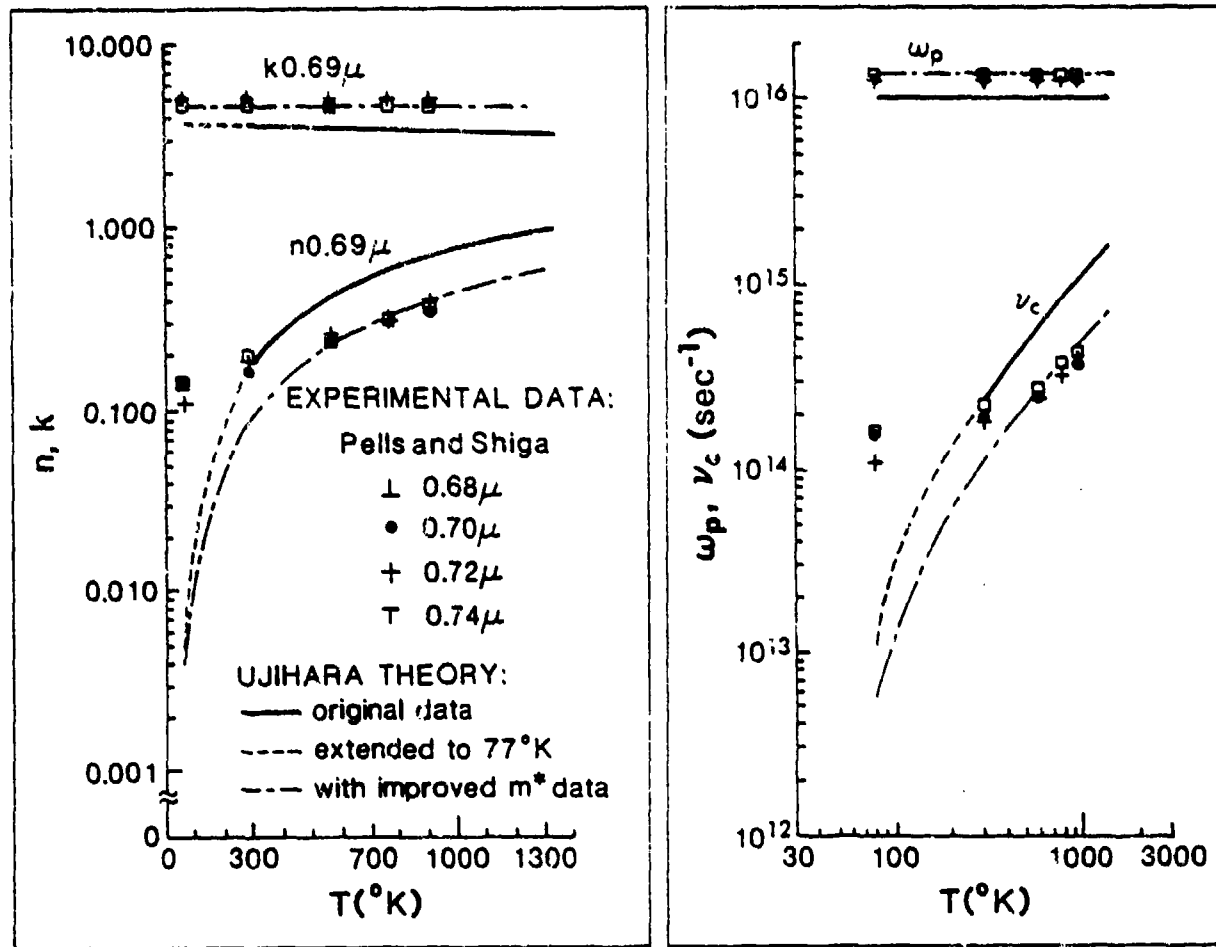


Fig. 6. Temperature dependence in copper of (a) optical material properties: index of refraction n and extinction coefficient k , and (b) free-electron material properties: plasma frequency ω_p and electron-phonon collision frequency ν_c .

IV. REFLECTANCE MEASUREMENTS

Other explanations for the reflectance behavior which is shown in Figure 1 fall into three categories: (1) a surface deformation which directs the reflected beam away from the detector, (2) plasma formation which absorbs or scatters the reflected light, or (3) a nonlinear process causing enhanced absorption within the metal. The first two categories involve processes which produce a reduction in light reaching the detector that could be misinterpreted as a decrease in the reflectance of the solid target surface. The importance of the first category, surface deformation, may be evaluated by comparing specular reflectance with total reflectance. The initial experiments of Bonch-Bruevich (Figure 1a) apparently measured total reflectance while those of Zavecz (Figure 1c) were specular reflectance measurements.

Experimentally, the reflectance of the metal surface is obtained by dividing the reflected pulse by the incident laser pulse. For a 30-ns laser pulse, even a time registration error as small as 1 ns between these two pulses can cause a significant error in the measured reflectance. This is indicated in Figure 7 where the solid pulse curve represents 30-ns FWHM Gaussian incident and reflected pulses, and the solid horizontal line is the corresponding reflectance. Time registration errors of 1 and 3 ns are shown by the dashed curves with the dashed reflected pulses now preceding the solid incident laser pulse. A shift of only 1 ns, corresponding to 3% of the width, can cause a reflectance error as high as 25% in the wings of the pulse shape.

To avoid a time registration error, we developed a method which uses a single detector for both pulses. A sample of the incident laser pulse is sent through an air delay path.¹¹ Both specular and total reflectance measurements have been carried out on copper targets. The experimental arrangement is sketched in Figure 8. A TRG model 104 ruby laser operating in the Q-switched mode produced 0.6J in a 30-ns FWHM pulse. A one to four beam expander reduced the measured beam divergence to ~1 mrad.

A high-intensity beamsplitter (Melles Griot Cat. No. 03 BTF 007 with 60% transmission at 6943 Å) provided a sample of the incident pulse. This sample pulse was delayed through an air path of ~20m for specular reflectance measurements and ~50m for total reflectance measurements.

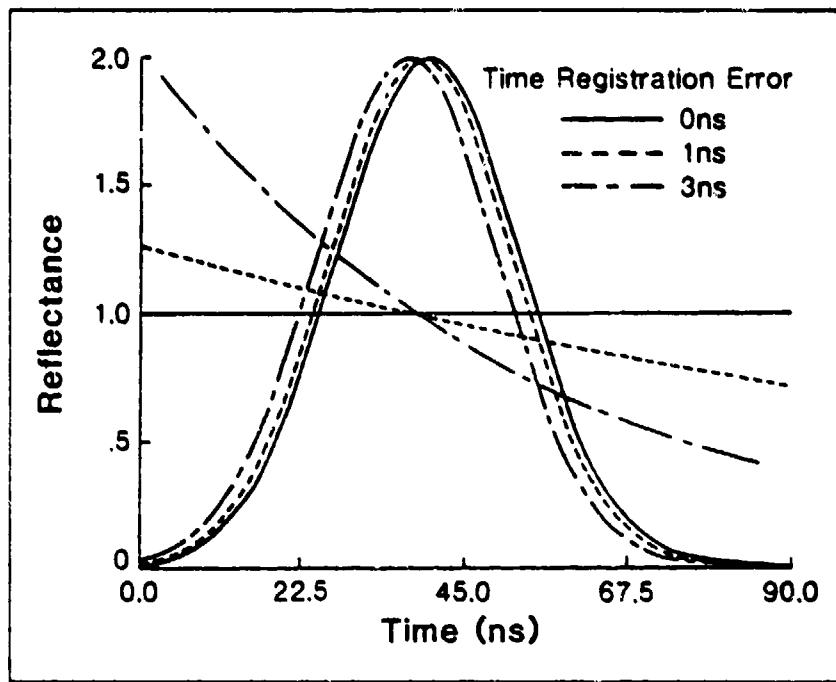


Fig. 7. Computed reflectance for 30-ns FWHM Gaussian reflected and incident laser pulses with 0, 1, and 3-ns time registration errors.

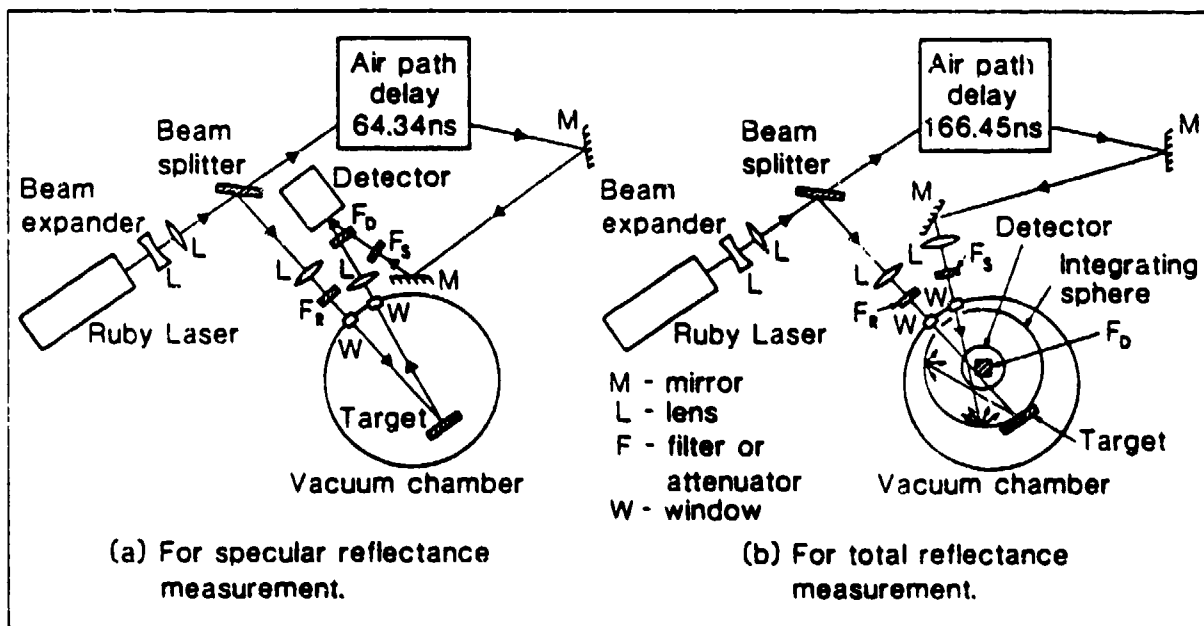


Fig. 8. Experimental arrangement. M = mirror, L = lens, F = filter or attenuator and W = window.

Both the reflected pulse from the target and the delayed sample incident laser pulse were detected by the same detector, a TRB 105B vacuum-photodiode with a detector area of 5 cm diam, a risetime < 0.3 ns and a dc-1.25 GHz bandwidth. The detector output was coupled to a Tektronix 519 oscilloscope which has a dc-1 GHz bandwidth. Therefore, the resolution of the detected light signal was ~ 0.5 ns.

The copper target surfaces were produced by vacuum-deposition on a glass plate of good optical quality. Evaporation and rf sputtering have each been used to produce copper films ~ 2000 Å thick. The sputtered copper deposit exhibited stronger adhesion to the glass base-plate than did the evaporated coating. Following vacuum deposition, the copper deposit on the glass plate was backed up by electroplating to produce a mechanically-strong copper target a few mm thick. Thus prepared, the copper target was kept attached to the glass plate until required for the reflectance measurements. Then the glass was detached and the vacuum-deposited copper target placed in the vacuum chamber. In this way an oxide-free copper surface could be prepared and protected until the measurements were taken. As indicated in Figure 8, the targets were located in a vacuum chamber, and a mechanical pump reduced the chamber pressure below 0.1 Torr to avoid air breakdown at the target surface.

The specular reflectance measurements are indicated in Figure 8a. The 40% reflected beam from the beamsplitter was focused onto the target with a 50-cm focal length 15-cm diam quartz lens. At the focused spot ~ 0.5-mm diam a maximum intensity of 10^9 W/cm^2 was obtained without any filters. This was determined from a measured energy of 75mJ on the target. Corning glass filters were used as attenuators to adjust incident reflected and detected intensities. Four aluminized mirrors were used to provide an air path delay of ~ 65 ns for the sample of the incident laser pulse.

In the total reflectance measurements, an integrating sphere was used as indicated in Figure 8b. The sphere was fabricated from two plastic hemispheres of 20 cm i.d. which were coated with Eastman White Reflectance Coating.²⁴ The Eastman Coating, a composition of barium sulphate, binder and solvent, is characterized by high reflectance, high stability and nearly-perfect diffuse reflection. The manufacturer's specifications²⁵ show .992 reflectance at 7000 Å. Not only does an integrating sphere carry out a

spatial integration of the light reflected from a target surface, but it delays the arrival of light at the detector by varying times depending on the path within the sphere. Thus the temporal shape of the detected light signal may be significantly modified. A 30-ns FWHM ruby laser pulse reflected from a metal target surface onto the 20 cm diam integrating sphere was lengthened by ~ 10 ns when measured by the fast vacuum photodiode located at the top of the sphere. The pulse lengthening is in good agreement with the theory of the integrating sphere for pulsed light sources.²⁶ Both the reflected pulse and the sample laser pulse were directed into the integrating sphere for the total reflectance measurements. Because of the pulse-lengthening property of the integrating sphere, a longer air delay path, ~ 50 m, was required to avoid overlapping the reflected and sample laser pulses. After the air path delay, as shown in Figure 8b, the sample of the incident laser pulse was sent through a second entrance window directly onto the integrating sphere surface; however, it was not focused on the sphere.

For each reflectivity measurement, a Polaroid picture was taken of the Tektronix 519 oscilloscope trace showing a reflected pulse followed by a sample incident laser pulse. To facilitate data analysis the pictures were enlarged by a linear factor of ~ 6, as shown in Figure 9.

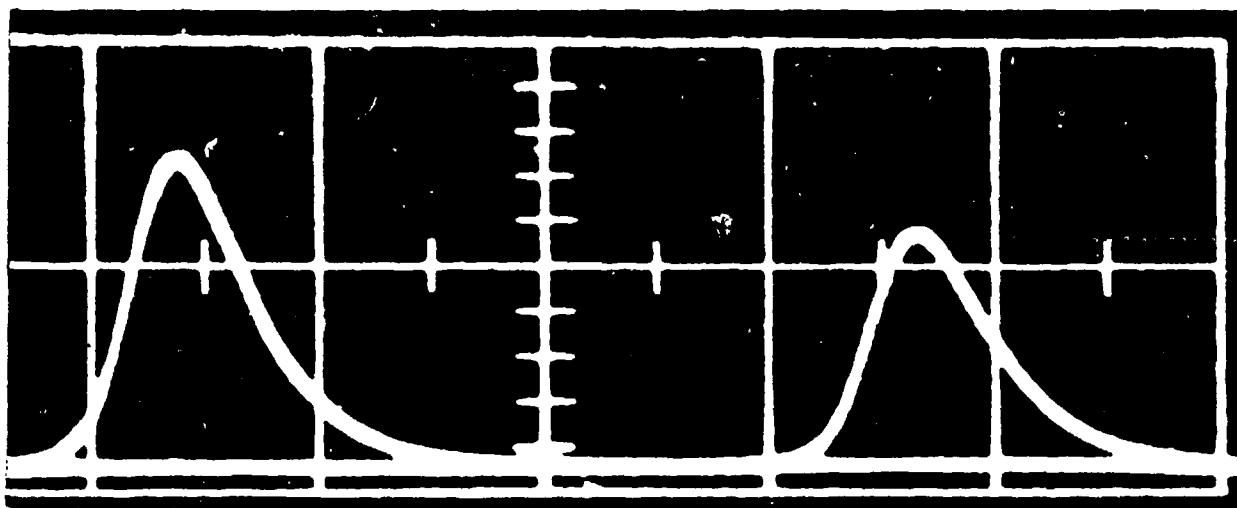


Fig. 9. Enlargement of an oscilloscope trace showing the specularly-reflected pulse from an evaporated-copper target surface and a sample of the incident $3.15 \times 10^8 \text{ W/cm}^2$ ruby laser pulse. The horizontal time scale is 50 ns/large division.

Readings were taken at 2mm intervals of both the upper and lower boundaries of the thickened curve trace. Approximately 90 upper and lower curve trace values were entered into a PDP 11/60 minicomputer as two vectors. An interactive graphic language was then used to average the two vectors, remove the time delay of the sample laser pulse, divide the reflected pulse by the sample laser pulse, apply the calibrated scale factor to change from relative to absolute reflectance and, finally, display the reflectance curve. The calibration factor involved filter, window and lens transmissions, mirror reflectivities in the air delay path and the beamsplitter transmission and reflection. For incident laser pulses within a narrow range of intensity, the reflectance curves were averaged and examples are presented in Figure 10 for specular reflectance and in Figure 11 for total reflectance of a vapor-deposited copper surface for three incident laser power

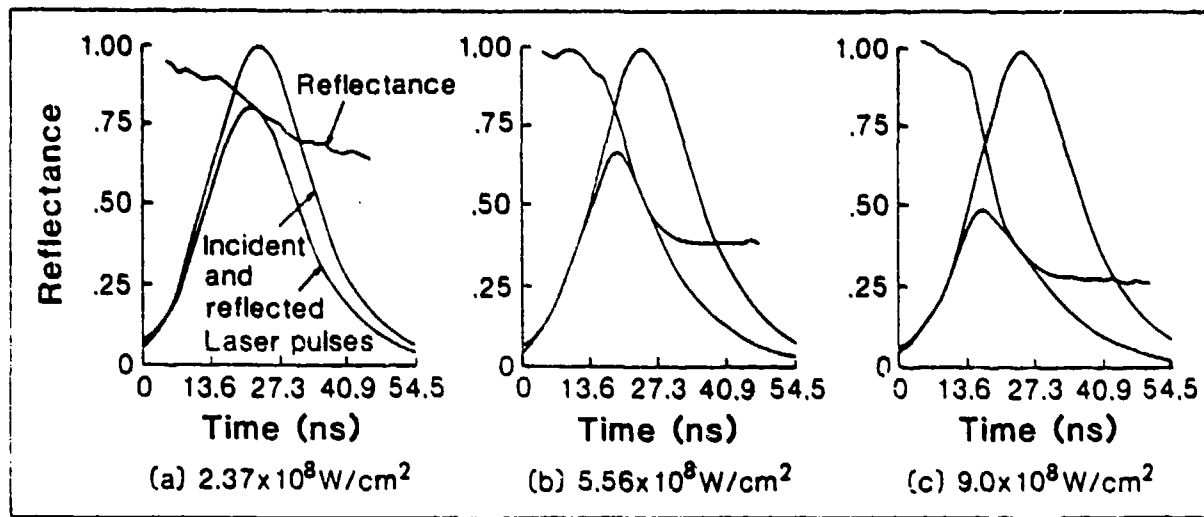


Fig. 10. Specular reflectance of copper.

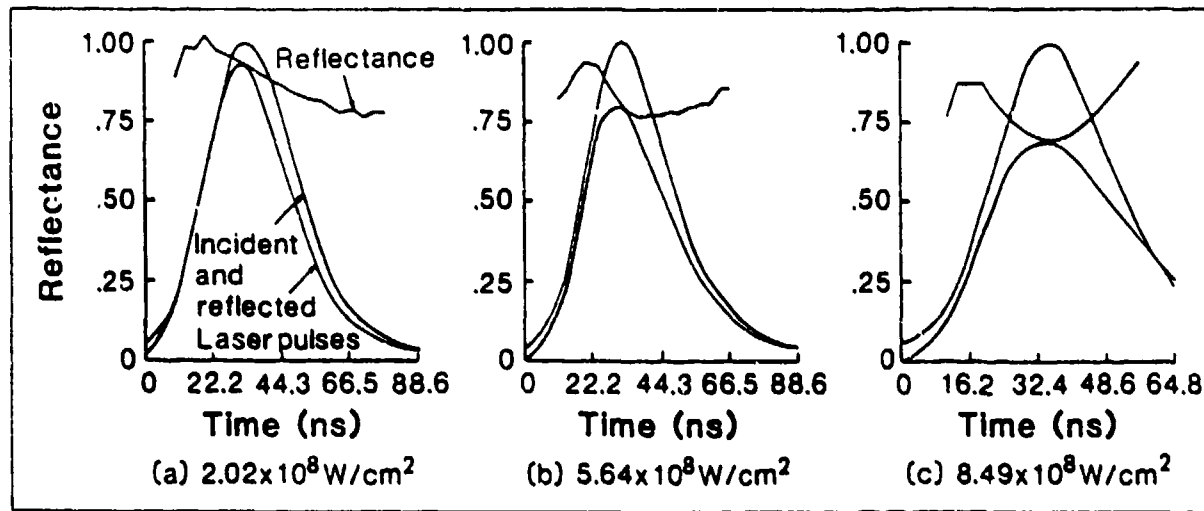


Fig. 11. Total reflectance of copper.

densities, ~2, 5, and 9×10^8 watts/cm². The curves shown are a normalized incident laser pulse, the reflected pulse and the metal target's reflectance behavior which is the ratio of the two pulse curves. The laser energy absorbed was calculated from these results and the temperature history of the metal surface determined using a one-dimensional heat-conduction approach as described in Section V.

V. TEMPERATURE OF THE METAL SURFACE

When laser radiation strikes a metal surface, the light not reflected is absorbed in a thin layer $10^{-6} - 10^{-5}$ cm thick. The energy is absorbed by electrons which equilibrate with the lattice vibrations in a time $\ll 10^{-9}$ sec. For nanosecond or longer laser pulses, therefore, the laser radiation absorbed may be considered to be immediately converted into heat and available for conduction into the metal. For a laser pulse of ~ 30 ns duration, the thickness of the region heated during the laser pulse is $\sim \sqrt{\kappa t}$ or 10^{-4} cm which is very small compared with the thickness of the usual metal target. (κ is the thermal diffusivity, $0.91 \text{ cm}^2/\text{sec}$ for copper.) Therefore, the absorbed energy may be treated as a surface heat source propagating into a metal of semi-infinite dimensions. The heat flow equation is:

$$\frac{\partial T(\underline{r}, t)}{\partial t} = \kappa \nabla^2 T(\underline{r}, t) + \frac{\alpha q_o(\underline{r}, t)}{\rho c_p} e^{-\alpha z} \quad (1)$$

where T is the temperature of the metal as a function of position on the surface \underline{r} and time t ; κ is the diffusion coefficient, ρ the density of the metal, c_p the specific heat of metal at constant pressure, α the attenuation coefficient and $q_o(\underline{r}, t)$ is the intensity of the absorbed laser radiation on the surface. The dimension z is the moving coordinate into the metal perpendicular to the surface, and $z=0$ is the boundary surface on which laser radiation is incident. The boundary conditions are $dT/dz = 0$ for $z \leq 0$, that is, no return heat flow, and $T(z \rightarrow \infty, t) = T_o$. The initial condition is $T(\underline{r}, 0) = T_o$ where T_o is the ambient temperature. We shall assume a Gaussian spatial intensity distribution of the absorbed laser radiation

$$q_o(\underline{r}, t) = \frac{P(t)}{\pi w^2} e^{-\left(\frac{r}{w}\right)^2} = q(t) e^{-\left(\frac{r}{w}\right)^2} \quad (2)$$

where $P(t)$ is the power absorbed from the incident radiation, w is the radius of the irradiated spot and r is the distance from the beam axis on the surface plane. Since the attenuation coefficient is very large ($\alpha \sim 10^5 - 10^6 \text{ cm}^{-1}$), or equivalently, the skin depth $\sqrt{2/\alpha \mu \sigma}$ is very small, the absorbed energy can be regarded as a surface heat source, i.e., $\alpha e^{-\alpha z} \rightarrow \delta(z)$ for large α . In cylindrical coordinates (r, ϕ, z) , Eq. (1) becomes

$$\frac{\partial T(r, z, t)}{\partial t} = \frac{k}{r} \frac{\partial}{\partial r} r \frac{\partial T}{\partial r} + k \frac{\partial^2 T}{\partial z^2} + \frac{1}{\rho c_p} \frac{P(t)}{\pi w^2} e^{-\left(\frac{r}{w}\right)^2} \delta(z) \quad (3)$$

with the boundary and initial conditions already given.

The Green's function for the heat flow equation in a semi-infinite conductor with a surface source having a spatial Gaussian heat distribution, i.e., the solution of the heat conduction equation for a unit input of the form

$$\frac{1}{\pi w^2} e^{-\left(\frac{r}{w}\right)^2} \delta(t) \delta(z) \quad , \quad (4)$$

is shown in References 27 and 28 to be

$$G(r, z, t) = \frac{1}{\pi^{3/2} \rho c_p \sqrt{k} t (w^2 + 4kt)} e^{-\frac{z^2}{4kt}} e^{-\frac{r^2}{w^2 + 4kt}} \quad . \quad (5)$$

The solution of Eq. (3) for absorbed power $P(t)$ is given by the time convolution of the Green's function and $P(t)$.

$$T(r, z, t) = T_0 + \int_0^t G(r, z, t-t') P(t') dt' \quad . \quad (6)$$

Thus,

$$T(r, z, t) = T_0 + \frac{1}{\sqrt{\pi}} \int_0^t \frac{1}{\rho c_p \sqrt{k}} \frac{z^2}{\sqrt{t-t'}} e^{-\frac{z^2}{4k(t-t')}} e^{-\frac{r^2}{w^2 + 4k(t-t')}} dt' \quad (7)$$

where

$$q(t) = \frac{P(t)}{\pi w^2} \approx \frac{P(t)}{\pi [(w^2 + 4k(t-t'))]}$$

since $w \gg \sqrt{4kt}$ for $w \approx 0.1$ cm, $k \approx 1$ cm²/sec and $t \approx 100$ nsec. The temperature of the metal surface $T(t) = T(0, 0, t)$ is

$$T(t) = T_0 + \int_0^t \frac{1}{\sqrt{\pi \rho c_p k}} \frac{q(t')}{\sqrt{t-t'}} dt' \quad (8)$$

where $K = \rho c_p K$ is the thermal conductivity of the metal. In the presence of energy loss mechanisms, such as melting, vaporization, etc., $q(t')$ is replaced by a net heat input $f(t') = q(t') - l(t')$. The loss term $l(t)$ represents all heat loss processes besides conduction and is treated as a function of the surface temperature, i.e., $l[T(t)]$. For convenience, a Gaussian spatial loss distribution has been assumed. Thus, the general expression for $T(t)$ is given by

$$T(t) = T_0 + \int_0^t \frac{1}{\sqrt{\pi \rho c_p K}} \frac{f(t')}{\sqrt{t-t'}} dt' \quad (9)$$

Not only is the solution given by Eq. (9) more compact than a LaPlace transform solution, but Eq. (9) also has a clear physical interpretation since $f(t)\sqrt{Kt}$ represents the energy absorbed in the affected volume and $1/\rho c_p$ is the specific heat factor which converts the absorbed energy to a temperature change. Moreover, the integration in Eq. (9) can easily be carried out for any function $f(t)$ provided the function $f(t)$ can be approximated by a polynomial expansion in t for each region of the integration interval.

As the incident laser radiation is absorbed, the surface temperature of the metal increases until it reaches the melting point. Then while the metal absorbs the energy corresponding to the latent heat of fusion the surface temperature remains constant. The thickness of the molten layer depends on the intensity of the absorbed laser radiation and on the thermal properties of the metal. After a molten surface layer is formed, the temperature of the liquid metal increases further until substantial vaporization occurs. An appreciable amount of the absorbed energy is then spent in supplying the evaporation energy and excess kinetic energy of the vapor which significantly reduces the surface heating rate. Unless the vapor has a low ionization energy, the vapor cloud remains transparent to the incident beam. On the other hand, the resultant high vapor pressure exerts a force on the molten layer under the irradiated spot. When the tangential shear force due to the high vapor pressure exceeds the surface tension of the liquid metal, the molten layer starts to move out of the irradiated zone. At this point perhaps it should be noted that the effects of radiation pressure of the incident beam for the laser pulses considered ($10^7 - 10^9 \text{ W/cm}^2$; $\sim 30 \text{ nsec FWHM}$), and the surface tension gradients on the molten layer arising from the non-uniform temperature distribution due to the Gaussian laser-beam intensity distribution assumed across the irradiated region are smaller by many

orders of magnitude than the effects of high vapor pressure.

When liquid metal is removed from the irradiated zone, part of the absorbed laser energy is required to melt and heat the surface of the freshly exposed spot to the temperature of the departed surface layer. From the point of view of an observer in a coordinate system located on the metal surface, the ejection of liquid metal slows the conductive heating process.

When the intensity of the absorbed laser radiation is high enough ($\geq 10^9 \text{ W/cm}^2$) for the metal surface temperature to increase beyond the boiling point of the metal, the incoming laser radiation may interact with the dense vapor cloud in front of the surface. Now the reflection of the incident beam takes place in a region with a gradual change of density, and consequently of refractive index, instead of at the sharp boundary between two distinct phases. At this point the absorption mechanism of the incident laser radiation is switched from the metal surface to the dense vapor layer in front of the metal. A further increase of the vapor temperature can result in appreciable excitation, ionization, and plasma formation. The plasma can now increase the coupling between the laser radiation and the metal surface. Later, when the plasma moves away from the metal target surface, a decoupling will take place.

Temperature histories were determined²⁹ for the metal targets using Eq. (9). The laser power absorbed, $q(t)$, was determined from the measured incident laser pulse and the measured total reflectance (e.g. Fig. 11). Heat-loss processes in addition to conduction, $\ell(t)$, were treated as a function of temperature and terms were included for melting, vaporization, expulsion of liquid metal and solidification in the appropriate temperature regions. The thermal conductivity and specific heat were also changed from measured values for the solid to those for the liquid in the appropriate temperature region. The integration of Eq. (9) was carried out using a trapezoidal approximation and an iterated substitution method. Table 2 gives the temperature histories for the three ruby laser - copper target interactions whose reflectances were measured in Figure 11. Surface temperatures above the boiling point of copper, 2840°K , are probably excessive because additional loss mechanisms such as absorption by the dense vapor layer and plasma formation are not included in this calculation.

Table 1. Calculated surface temperature at the center of the interaction site irradiated by a ruby laser pulse producing 2.02, 5.64 and $8.49 \times 10^8 \text{ W/cm}^2$ on a copper target.

TIME [nsec]	COPPER SURFACE TEMPERATURE		
	2.02 MW/cm	5.64 MW/cm ²	8.49 MW/cm ²
0	300°K	300°K	300°K
5	312°K	343°K	346°K
10	333°K	483°K	464°K
15	378°K	784°K	910°K
20	475°K	1236°K	1577°K
25	640°K	2373°K	4841°K
30	811°K	3730°K	7869°K
35	955°K	4247°K	8697°K
40	1040°K	4255°K	8289°K
45	1040°K	3966°K	7484°K
50	1012°K	3606°K	6636°K
55	971°K	3368°K	5849°K
60	912°K	3202°K	5227°K
65	851°K	3037°K	4743°K
•			
•			
•			
130	572°K		2352°K

VI. DISCUSSION

The measured total reflectances of evaporated-copper target surfaces show a slow decrease with increasing incident laser intensity or increasing surface temperature up to the boiling point of the metal. At low incident laser power densities (i.e., $< 3 \times 10^8 \text{ W/cm}^2$) the specular and total reflectances of the metal target surface are similar (cf. Figure 10a with Figure 11a). The one-dimensional heat-conduction calculations indicate that the copper surface did not reach the melting point with this incident laser power density; namely, $2 \times 10^8 \text{ W/cm}^2$. No permanent damage was observed in the copper. The copper target was examined under 200x magnification and no trace of melting was observed. The lack of any permanent observable damage is consistent with the calculated maximum surface temperature of 1040°K and with the equality of the specular and total reflectances.

At an incident laser power density of $5.6 \times 10^8 \text{ W/cm}^2$, the specular reflectance undergoes a sharp drop which is not observed in the total reflectance (cf. Figure 10b with Figure 11b). The one-dimensional heat-conduction calculation indicates that the maximum temperature attained by the copper surface was in excess of the boiling point. Permanent damage was observed at the interaction site. Once again the permanent changes observed in the target are consistent with the surface temperatures calculated and the reflectances measured which reveal a decrease in the specular accompanied by an increase in the diffuse component of the reflectance.

An additional increase in incident laser power density to $\sim 9 \times 10^8 \text{ W/cm}^2$ continues the decrease in specular reflectance (Figure 10c compared with 10b). Permanent target surface damage is more severe and the crater site is more extensive. The recovery in the total reflectance behavior which is evident in Figure 11c is caused by a "light flash" produced by emission of light from a plasma that is formed at or in front of the metal surface. The spectral content of this light includes sharp emission lines from neutral copper atoms, copper ions and copper dimers (Cu_2 molecules).³⁰

When an interference filter is inserted in front of the TRB 105B vacuum photodiode thereby restricting the light detected to $\pm 50^\circ\text{A}$ around the 6943°A ruby laser wavelength, then the recovery in total reflectance behavior so evident in Figure 11c and just noticeable in Figure 11b disappears.³⁰

VII. PROBE LASER REFLECTANCE MEASUREMENTS

When light from the high-power laser pulse is used to provide the optical measurement of target reflectance, the signal is only present and hence the reflectance measurement can only be carried out during the short time period of the laser pulse length. During the initial portion of the rise-time and the final portion of the trailing edge of the laser pulse, the signal-to-noise ratio of the reflectance measurement deteriorates. Thus, precise reflectance measurement can only be made for a time period somewhat greater than the FWHM which was ~ 30 ns for the ruby laser used in our experiments. If a cw probe laser were focused to a spot on the target which is entirely within the focused spot of the ruby laser, then a second set of reflectance measurements could be taken using the cw probe laser. Probe laser reflectance measurements would provide two types of additional information to assist in our understanding of the processes involved: 1) reflectance measurements over much longer time periods, and 2) reflectance measurements at a second wavelength. Reflectance measurements over longer time periods would provide more sensitive measurements during the initial stage when the high-power laser is turning on as well as through the maximum target surface temperature period as the high-power laser is turning off and also into the cooling region as the surface resolidifies. Reflectance measurements at a second wavelength can also be important in identifying the role of nonlinear processes in accounting for the steep reflectance drop shown in Figure 1. Both reflectances would be expected to be the same except when a nonlinear process such as enhanced absorption causes a decrease in reflectance at the high-power laser frequency but not necessarily also at a second, non-resonant low-power probe laser frequency.

The 6328 \AA helium-neon laser is a readily available cw probe laser. It is close enough to the 6943 \AA ruby laser to produce nearly the same response from our detection system and is also close enough to avoid exciting inter-band transitions in targets like copper. In addition, the visible output facilitates the alignment of its focused spot to ensure that it is entirely within that of the ruby high-power laser. The 615 \AA separation between the two laser wavelengths is sufficient for easy discrimination by ordinary 100 \AA commercial interference filters. To separate the signal from a 1 mW He-Ne laser from a 10 MW ruby laser pulse, we had expected to use a stack

of four interference filters since the skirt-to-peak transmission ratio of a single interference filter is generally 10^{-3} to 10^{-4} .

When this type of probe reflectance measurements were attempted, we discovered, unfortunately, that enough direct ruby light or fluorescence produced by the ruby light was received at the detector to overwhelm the 6328 \AA probe laser signal. A light-tight holder to accommodate a sequence of alternate filters and apertures was constructed to prevent any light from reaching the detector by paths through the edges or around the filters. Even when the number of filters in the stack was increased to nine to overcome possible bleaching in the first few filters, a direct pulse was still detected from the ruby laser. We concluded that mechanisms such as bleaching or fluorescence produced by the high-power ruby pulse prevented adequate discrimination by a stack of interference filters.

Liquid solutions were also examined. The smallest ratio of transmission at 6943 \AA to transmission at 6328 \AA achieved was 0.05. This was produced by the Q-switch solution of cryptocyanine in acetonitrile (Eastman A10220) but was far from what was required to provide adequate discrimination between the two lasers.

We were able to carry out specular reflectance measurements³¹ using a He-Ne probe laser when a Jarrell-Ash 0.5 m Ebert spectrometer with a single 6328 \AA interference filter in front of the entrance slit was used to provide wavelength discrimination. Even with this arrangement a small light pulse was detected when the He-Ne probe laser was turned off. While the specularly reflected beam is collimated and can be focused into the acceptance angle of a spectrometer, the output beam from the integrating sphere has a 2π steradian solid angle and too great a light loss to utilize a spectrometer in carrying out total reflectance probe-laser reflectance measurements.

Alternate approaches are: 1) use a dye laser with greater power output and somewhat greater separation from the 6943 \AA ruby laser, or 2) choose a probe laser whose wavelength is longer than the ruby such as a cw YAG at $1.06\text{ }\mu$. Then cut-on transmission filters would provide much easier discrimination against the higher-power but now shorter wavelength ruby laser. One problem with this second approach is that the probe laser beam would not be visible and there would be much greater difficulty insuring that its focused spot was entirely within the focused ruby spot.

VIII. CONCLUSIONS

Thus far we may conclude that specular reflectance is a sensitive indicator of surface deformation. On the other hand, total reflectance measurements show that until the surface temperature of a metal target reaches the vicinity of the boiling point, no significant deviation is observed in the reflectance from that given by a Drude free-electron model. These results are in agreement with those of von Allmen et al.⁹ but contradict the conclusions of other workers that a decrease of ~ 50% in the total reflectance occurs at or possibly even before the melting point of a metal surface is reached.

A most important result has been the preliminary verification of our initial postulate — that direct, real-time measurements of the target material's optical properties with subnanosecond resolution can provide crucial, process-revealing signatures in following the interaction of an intense laser beam with a metal as the surface progressively undergoes heating, plastic deformation, slip, vaporization, ejection of liquid metal, plasma formation, etc. Measurement of the target's optical properties should be continued along with spectroscopic measurement of the plasma generated. Electron and target species densities and temperatures can be compared with recent theoretical results.³² In this way our understanding of the laser-material interactions will improve and the high-power densities available from lasers can be more fully utilized in a wide variety of material processing applications.

IX. REFERENCES

1. A. M. Bonch-Bruevich, Ya. A. Imas, G. S. Romanov, M. N. Liebenzon and L. N. Mal'tsev, "Effect of a Laser Pulse on the Reflecting Power of a Metal," Sov. Phys. -Tech. Phys., 13 (1968) pp. 640-643.
2. N. G. Basov, V. A. Boiko, O. N. Kroklin, O. G. Semenov and G. V. Sklizkov, "Reduction of Reflection Coefficient for Intense Laser Radiation on Solid Surfaces," Sov. Phys. -Tech. Phys., 13 (1969) pp. 1581-1582.
3. A. M. Prokhorov, V. A. Batanov, F. V. Bunkin and V. B. Federov, "Metal Evaporation under Powerful Optical Radiation," IEEE J. Quantum Electronics, QE-9 (1973) pp. 503-510.
4. T. E. Zavecz, M. A. Saifi and M. Notis, "Metal Reflectivity under High-Intensity Optical Radiation," Appl. Phys. Lett., 26 (1975) pp. 165-168.
5. J. C. Koo and R. E. Slusher, "Diffraction from Laser-Induced Deformation on Reflective Surfaces," Appl. Phys. Lett., 28 (1976) pp. 614-616.
6. J. F. Ready, "Change of Reflectivity of Metallic Surfaces During Irradiation by CO₂-TEA Laser Pulses," IEEE J. Quantum Electronics, QE-12 (1976) pp. 137-142.
7. P. W. Chan, Y. W. Chan and H. S. Ng, "Reflectivity of Metals at High Temperatures Heated by Pulsed Laser," Phys. Lett., 61A (1977) pp. 151-153.
8. Yu. I. Dymshits, "Reflection of Intense Radiation from a Thin Metal Film," Sov. Phys. -Tech. Phys., 22 (1977) pp. 901-902.
9. M. von Allmen, P. Blaser, K. Affolter and E. Stürmer, "Absorption Phenomena in Metal Drilling with Nd-Lasers," IEEE J. Quantum Electronics, QE-14 (1978) pp. 85-88.
10. C. T. Walters and A. H. Clauer, "Transient Reflectivity Behavior of Pure Aluminum at 10.6 μ m," Appl. Phys. Lett., 33 (1978) pp. 713-715.
11. K. Park and W. T. Walter, "Reflectance Change of a Copper Surface During Intense Laser Irradiation," pp. 274-282 in Proceedings of the International Conference on LASERS '78, V. J. Corcoran, ed.; Orlando, Florida, December 1978, and "Metal Reflectance Changes During Intense Laser Irradiation," pp. 21-31 in Applications of Lasers in Materials Processing, E. A. Metzbower, ed.; American Society for Metals, Metals Park, Ohio, 1979.

12. N. F. Mott and H. Jones, The Theory of the Properties of Metals and Alloys, Clarendon Press, Oxford, England (1936).
13. K. Ujihara, "Reflectivity of Metals at High Temperature," J. Appl. Phys., 43 (1972) pp. 2376-2383.
14. N. F. Mott and H. Jones, op cit p. 116.
15. G. Hass et al., 1965, as quoted in American Institute of Physics Handbook, D. E. Gray, ed.; McGraw Hill, New York (1972) pp. 6-157.
16. N. F. Mott and H. Jones, op cit p. 278.
17. W. T. Walter, "Reflectance Changes of Metals During Laser Irradiation," pp. 109-117 in Laser Applications in Materials Processing, J. F. Ready and C. B. Shaw, Jr., ed.; Proc. of SPIE, 198 (1980).
18. K. Forsterling and V. Fredericksz, Ann. Physik, (1913) 40 p. 200, as quoted in M. P. Givens, "Optical Properties of Metals," p. 324 in Solid State Physics 6 Academic Press, New York (1958).
19. G. P. Pells and M. Shiga, "The Optical Properties of Copper and Gold as a Function of Temperature," J. Phys. C. (Solid St. Phys.), 2 (1969) pp. 1835-1846; and G. P. Pells, n and k data furnished by private correspondence as indicated in this reference.
20. L. G. Schulz, "An Experimental Confirmation of the Drude Free Electron Theory of the Optical Properties of Metals for Silver, Gold and Copper in the Near Infrared," J. Opt. Soc. Am., 44 (1954) pp. 540-545.
21. K. Weiss, Z. Naturforsch, 3a (1948) p. 143, as quoted in American Institute of Physics Handbook, D. E. Gray, ed.; McGraw Hill, New York (1972) pp. 6-133.
22. S. Roberts, Phys. Rev., 118 (1960) p. 1509, as quoted in American Institute of Physics Handbook, D. E. Gray, ed.; McGraw Hill, New York (1972) pp. 6-133.
23. F. P. Gagliano and V. J. Zaleckas, "Laser Processing Fundamentals," p. 146 in Lasers in Industry, S. S. Charschan, ed.; Van Nostrand Reinhold, New York (1972).
24. Eastman White Reflectance Coating, Catalog No. 6080, Eastman Kodak Co., Rochester, New York 14650. In order to have an adequate thickness of the coating, the inside surfaces of the two hemispheres were sprayed four to eight times using a Kodak Laboratory Sprayer, Catalog No. 13270.

25. Eastman White Reflectance Coating, Kodak Publication No. JJ-32, Rochester, New York (1976); and F. Grum and G. W. Luckey, "Optical Sphere Paint and a Working Standard of Reflectance," *Appl. Optics* Vol. 7, pp. 2289-2294, 1965.
26. K. Park and W. T. Walter, "Theory of the Integrating Sphere for Pulsed Light Sources," Appendix A of K. Park, "Change in the Reflectivity of a Metal Surface during Intense Laser Irradiation," Ph.D. Thesis, Polytechnic Institute of New York, 1978.
27. H. S. Carslaw and J. C. Jaeger, "Conduction of Heat in Solids," 2nd Ed., Oxford University Press, London, 1959.
28. C. Bar-Isaac and U. Korn, "Moving Heat Source Dynamics in Laser Drilling Processes," *Appl. Phys.* Vol. 3, pp. 45-54, 1974.
29. K. Park, "Change in the Reflectivity of a Metal Surface during Intense Laser Irradiation," Ph.D. Thesis, Polytechnic Institute of New York, 1978.
30. W. T. Walter, N. Solimene, K. Park, T. H. Kim and K. Mukherjee, "Optical Properties of Metal Surfaces during Laser Irradiation," in Lasers in Metallurgy, TMS-AIME Conference Series (to be published 1981).
31. To Hoan Kim, "High-Energy Pulsed Laser Interaction with Metallic Surfaces," Ph.D. Thesis, Polytechnic Institute of New York, 1980.
32. M. Newstein and N. Solimene, "Laser Metal Interaction in Vacuum," *IEEE J. Quantum Electron.* (to be published September 1981).

X. LIST OF PUBLICATIONS AND DISSERTATIONS

1. Kyunglin Park, "Change in Reflectivity of a Metal Surface During Intense Laser Irradiation," Ph. D. Thesis, Polytechnic Institute of New York (June 1978).
2. K. Park and W. T. Walter, "Reflectance Change of a Copper Surface During Intense Laser Irradiation," Proceedings of the International Conference on LASERS '78, pp. 274-282, Orlando, Florida (December 1978).
3. K. Park and W. T. Walter, "Metal Reflectance Changes During Intense Laser Irradiation," Applications of Lasers in Materials Processing; Materials/Metalworking Series (E. A. Metzbower, editor), American Society for Metals, Metals Park, Ohio, pp. 21-31 (1979).
4. K. Mukherjee, T. H. Kim and W. T. Walter, "Nature of High Energy Pulse Laser Induced Melting in Sn, Zn and Bi," Microstructure and Properties of Rapidly solidified Non-Ferrous Metals Symposium, Metallurgical Society of AIME, Vol. 31, p. F-19, September 1979.
5. William T. Walter, "Reflectance Changes of Metals During Laser Irradiation," Proc. of Soc. of Photo-Optical and Instrumentation Engineers, Vol. 198 (J. F. Ready and C. B. Shaw, editors) pp. 109-117 (1980).
6. To Hoon Kim, "High-Energy Pulsed Laser Interaction with Metallic Surfaces," Ph. D. Thesis, Polytechnic Institute of New York, June 1980.
7. K. Park and W. T. Walter, "Theory of the Integrating Sphere for Pulsed Light Sources," (accepted for publication in the Journal of the Optical Society).
8. K. Mukherjee, T. H. Kim and W. T. Walter, "Shock Deformation and Microstructure in Laser Induced Damage in Metals," (invited paper presented at AIME Annual Meeting, to be published in Lasers in Metallurgy, TSM-AIME Conference Series, 1981).
9. W. T. Walter, N. Solimene, K. Park, T. H. Kim and K. Mukherjee, "Optical Properties of Metal Surfaces During Laser Irradiation," (invited paper presented at AIME Annual Meeting, to be published in Lasers in Metallurgy, TSM-AIME Conference Series, 1981).

XI. LIST OF PERSONNEL INVOLVED IN RESEARCH

William T. Walter, Principal Investigator, Department of Electrical Engineering and Microwave Research Institute.

Kalinath Mukherjee, Department Head, Department of Physical and Engineering Metallurgy and Microwave Research Institute.

Nathan Marcuvitz, Institute Professor, Department of Electrical Engineering and Microwave Research Institute.

Maurice Newstein, Associate Professor, Department of Electrical Engineering and Microwave Research Institute.

Nicholas Solimene, Research Scientist, Department of Electrical Engineering and Microwave Research Institute.

Kyunglin Park, Ph.D. Candidate, Department of Electrical Engineering and Microwave Research Institute.

To H. Kim, Ph.D. Candidate, Department of Physical and Engineering Metallurgy and Microwave Research Institute.

William Woturski, Research Assistant, Microwave Research Institute.

Stanley Bielaczy, Research Assistant, Microwave Research Institute.

Robert DiFazio, Student Assistant, Department of Electrical Engineering and Microwave Research Institute.

XII. LIST OF COUPLING ACTIVITIES WITH OTHER PEOPLE AND GROUPS DOING RELATED RESEARCH

A. Meetings Attended:

1. International Conference on LASERS '78, Orlando, Florida, December 11 to 15, 1978.
 - a. William T. Walter was chairman of Session I on Materials and Interactions and presented a paper, "Reflectance Change of a Metal Surface During Intense Laser Irradiation," with K. Park.
 - b. Maurice Newstein presented a paper, "Kinetic Theory Treatment of Metal Evaporation Front," with N. Solimene and J. Hammer.
2. American Society for Metals Conference, "Applications of Lasers in Materials Processing," Washington, D. C., April 18-20, 1978.
 - a. William T. Walter presented a paper, "Metal Reflectance Changes During Intense Laser Irradiation," with K. Park.
 - b. Maurice Newstein presented a paper, "Structure of the Evaporation Front From Boltzmann Equation," with N. Solimene and J. Hammer.
3. Society of Photo Optical Instrumentation Engineers, Annual Meeting, San Diego, California, August 27-30, 1979.
 - a. William T. Walter presented an invited paper, "Reflectance Changes of Metals During Laser Irradiation," during the seminar "Laser Application in Materials Processing."
4. Metallurgical Society of the American Institute of Mining, Metallurgical and Petroleum Engineers, Fall Meeting, Milwaukee, Wisconsin, September 16-20, 1979.
 - a. Kalinath Mukherjee presented a paper, "Nature of High Energy Pulse Laser Induced Melting in Sn, Zn and Bi," during the symposium, "Microstructure and Properties of Rapidly Solidified Non-Ferrous Metals."
5. Eleventh International Quantum Electronics Conference, Boston, Massachusetts, June 23-26, 1980.
 - a. Maurice Newstein presented a paper, "Laser Metal Interaction in Vacuum."

B. Seminar Speakers at the Polytechnic

1. Dr. Alex Stein, Exxon Research Corporation, Linden, New Jersey, presented a seminar, "CF₄ Laser Research," on April 7, 1978.
2. Professor R. N. Sudan, Laboratory of Plasma Studies, Cornell University, Ithaca, New York, presented a seminar, "Two-Dimensional Turbulence in Low β Collisional Plasma," on May 19, 1978.
3. Dr. Richard L. Fork, Bell Telephone Laboratories, Holmdel, New Jersey, presented a seminar, "Dynamics of Photoexcited Gallium-Arsenide Band Edge Absorption with Subpicosecond Resolution," on July 7, 1978.
4. Dr. Sigrid McAfee, Bell Telephone Laboratories, Murray Hill, New Jersey, presented a seminar, "Nonlinear Absorption in Germanium on a Picosecond Time Scale," on August 4, 1978.
5. Dr. Raul Stern, Bell Telephone Laboratories, Murray Hill, New Jersey, presented a seminar, "New Results on Plasma Filamentation," on September 22, 1978.
6. Dr. N. J. Berg, Harry Diamond Laboratories, Adelphi, Maryland, presented a seminar, "Acousto-Optical Signal Processing," on October 12, 1978.
7. Professor Shalom Raz, University of Houston-Texas, presented a seminar, "An Open Problem in Inverse Scattering Theory," on February 23, 1979.
8. Dr. M. Keskinen, Naval Research Laboratory, Washington, D.C., presented a seminar, "Numerical Simulation of the Rayleigh-Taylor Instability," on March 9, 1979.
9. Professor C. Lee, Cornell University, Ithaca, New York, presented a seminar, "Laser Annealing," on March 30, 1979.
10. Dr. S. Basu, Air Force Geophysics Laboratory, presented a seminar, "Multi-Technique Observations of Equatorial Irregularities in the Night Time F-Region," on May 4, 1979.
11. Dr. E. McDonald, Naval Research Laboratory, presented a seminar, "Gradient-Drift Processes and Formation of Barium Cloud Striations," on May 18, 1979.
12. Dr. H. Eun, National Bureau of Standards, presented a seminar, "Gravity Waves and Atmospheric Species," on May 25, 1979.
13. Professor T. Shiosaki, Kyoto University, Japan, presented a seminar, "ZnO Thin Film for Bulk and SAW Applications," on August 3, 1979.
14. Professor I. Senitzky, The Technion, Israel, presented a seminar, "Cooperative Relaxation of a Coherently Driven Three Level System," on October 5, 1979.

15. Dr. Hyatt Gibbs, Bell Laboratories, Murray Hill, New Jersey, presented a seminar, "Optical Bistability," on January 11, 1980.
16. Professor Joel DuBow, Colorado State University, presented a seminar, "Automatic Network Analysis of Materials and Devices," on February 11, 1980.
17. Dr. M. Lax, Bell Laboratories, Murray Hill, New Jersey, presented a seminar, "Unstable Resonators in a Medium with Gain," on February 15, 1980.
18. Dr. S. McCall, Bell Laboratories, Murray Hill, New Jersey, presented a seminar, "Theory of Optical Bistability," on February 22, 1980.
19. Dr. Paul Rabinowitz, Exxon Research Laboratories, Linden, New Jersey, presented a seminar, "Controllable Pulse Compression in Raman Lasers," on June 6, 1980.